

Super light-by-light scattering in vacuum induced by intense vortex lasers

Zhigang Bu¹, Lingang Zhang¹, Shiyu Liu¹, Baifei Shen², Ruxin Li^{1,3}, Igor P. Ivanov^{4,*}, and Liangliang Ji^{1,†}

¹State Key Laboratory of High Field Laser Physics,

Shanghai Institute of Optics and Fine Mechanics (SIOM),
Chinese Academy of Sciences (CAS), Shanghai 201800, China

²Department of Physics, Shanghai Normal University, Shanghai 200234, China

³Shanghai Tech University, Shanghai 201210, China

⁴School of Physics and Astronomy, Sun Yat-sen University, Zhuhai 519082, China

(Dated: February 21, 2025)

Collision of ultra-intense optical laser and X-ray free electron laser (XFEL) pulses is a promising approach to detecting nonlinear vacuum polarization (VP), a long-standing prediction of quantum electrodynamics remaining to be tested. Identifying the signals induced by polarized vacuum relies on purifying the X-ray polarization and poses significant challenges due to strongly reduced signal and low signal-to-noise ratio (SNR). Here we propose an approach that allows one to directly detect VP signals without the need for an X-ray polarizer. We identify a new VP effect in collision of an X-ray probe with an intense laser in a vortex mode, which we call the super light-by-light scattering (super-LBL), through which signal photons are kicked out of the X-ray background with large tangential momentum. Super-LBL originates from the gradient force of the vortical vacuum current in azimuthal direction and induces momentum exchange beyond the transverse momentum of laser-photon. This effect efficiently sets the scattered signal photons apart from the X-ray background, producing observable signals with both the strength and SNR more than two orders of magnitude higher than those from the known VP effects. This finding paves the way for single-shot detection of nonlinear VP phenomena with current ultra-intense laser and XFEL technologies.

Introduction—According to Quantum Electrodynamics (QED), vacuum is filled with quantum fluctuations of virtual positron-electron pairs. Through these fluctuations, photon-photon interactions can occur even in vacuum. For this reason, vacuum exhibits weak anisotropic properties in the presence of strong electromagnetic fields and influences the photon propagation. This is known as nonlinear QED vacuum polarization (VP), first predicted by Heisenberg and Euler in 1936 [1]. Typical nonlinear QED VP effects include vacuum birefringence [2–4], light-by-light (LBL) scattering [5, 6], vacuum diffraction [7, 8], and generation of high-order harmonics and electromagnetic shock wave in vacuum [9, 10]. Their signal strengths scale as $\sim (I_L/I_{cr})^2$, where $I_{cr} = 2.1 \times 10^{29}$ W/cm² is the intensity of Schwinger critical field [11] and I_L is the intensity of the driving electromagnetic field.

With the present-day laser technology, the laser intensity achieved in laboratory has exceeded [12–15] 10^{22} W/cm² and is poised to reach [16] 10^{23} W/cm² soon. At the same time, X-ray Free Electron Laser (XFEL) facilities deliver high-flux, high-quality X-ray beams. It is increasingly promising to detect nonlinear QED VP by employing an ultra-intense laser as a driver and an X-ray as a probe [4, 16]. Nonetheless, with current laser technologies, the strength of VP signals is at least ten orders of magnitude lower than the probe X-ray background [4, 16, 17]. One is forced to produce enough signal photons and extract them from the X-ray background to significantly improve the signal-to-noise ratio (SNR).

There are two potential schemes to detect nonlinear VP effects. One is to rely on the vacuum birefringence effect [4, 18] and to detect polarization-flipped sig-

nal photons with the aid of an X-ray polarizer. As no more than 7% of the scattered photons are polarization-flipped [17], the birefringence signal photon count, even for $I_L = 10^{23}$ W/cm², drops to about 10^{-11} relative to the X-ray probe. Moreover, a high-resolution polarizer relies on multiple reflections of the X-ray beam in the polarizer crystal [19, 20]. This places strict requirements on the beam bandwidth and divergence angle [19, 21] and, at the same time, compromises the polarizer transmission efficiency, further attenuating the detectable signal by one order of magnitude. Dark-field detection [22] provides another method for enhancing the SNR and reducing the detection accuracy of the polarizer. However, it also reduces the probe photon number by blocking the central part of the X-ray beam before its focus. Adjusting the collision angle and transverse collision parameter of the driving laser and X-ray probe increases the divergence angle of the signal photon above that of the X-ray background [18], which may also relax the requirements for the detection accuracy of the X-ray polarizer.

The second scheme is to detect a signal from the LBL scattering, regardless of the photon polarization. The LBL signal strength is about 14 times higher than that of vacuum birefringence [17]. However, in the two-beam collision configuration (a driving laser vs. an X-ray probe), the energies and momenta of the scattered photons are almost unchanged, so that the signal photons cannot be identified without polarization measurements. This obstacle can be avoided in an oblique collision of an X-ray probe with two driving laser pulses [6, 23, 24]: the signal photons acquire a small transverse momentum (twice the transverse momentum of the driving lasers [24] in a symmetric setting), diverge from the X-ray background, and can be detected. As the collision angle increases, the

transverse momenta grow, but the signal strength drops by two orders of magnitude [17]. With additional challenges associated with experimental control of the three beam collision, detection of LBL scattering seems no easier than of vacuum birefringence. Further, with less than one detectable signal photon per shot and low SNR under the state-of-the-art laser technology, signal accumulation over multiple shots seems necessary, which imposes stringent requirements on the repetition rate of ultra-intense lasers. As a result, experimental detection of VP effects remains a major unresolved challenge.

In this work, we theoretically demonstrate that these challenges can be addressed in a novel VP effect, in which the nonlinear QED vacuum driven by an intense laser in a mixed vortex mode induces a surprisingly large transverse momentum kick to the scattered photons. We refer to this effect as the super light-by-light scattering (super-LBL). Super-LBL scattering steers the scattered photons out of the X-ray background and generates an observable signal with an SNR exceeding 100. This new effect is based on the counterpropagating two-beam collision and avoids the suppression of signals due to the large collision angle. Moreover, it does not depend on the X-ray polarization, eliminating the need for polarizers and the associated signal depletion. Thus, super-LBL scattering can produce more observable signal photons than the ordinary VP effects. We further demonstrate in a particle-in-cell (PIC) simulation that the driving laser in the mixed vortex mode can be generated using a custom-tailored double-ring spiral phase plate with the current experimental technologies. Our findings have significant advantages for detecting nonlinear QED VP effects, suggesting a promising experimental scheme with the present-day ultra-intense laser and XFEL technologies, and even allowing for single-shot measurements.

Theoretical model and demonstration—Nonlinear QED VP can be analyzed using Heisenberg-Euler Lagrangian density [1, 11], $\mathcal{L} = \mathcal{F} + 2\xi\mathcal{F}^2 + (7\xi/2)\mathcal{G}^2$, where the two Lorentz invariants of electromagnetic field are $\mathcal{F} = (\mathbf{E}^2 - \mathbf{B}^2)/2$ and $\mathcal{G} = \mathbf{E} \cdot \mathbf{B}$. Here, \mathbf{E} and \mathbf{B} are the total electric and magnetic fields, $\xi = \alpha/(45\pi E_{cr}^2)$ is the coefficient of vacuum polarization, $\alpha = 1/137$ is the fine structure constant, and $E_{cr} = 1.3 \times 10^{16}$ V/cm is the electric field strength of Schwinger critical field. In interaction of an intense laser pulse with an X-ray probe, polarization \mathbf{P} and magnetization \mathbf{M} are induced in vacuum and generate the equivalent current, $\mathbf{J}_V(t, \mathbf{x})$. This vacuum current in turn influences the X-ray probe and generates a $2 \rightarrow 2$ scattering process: an X-ray photon absorbs a laser photon and subsequently scatters into a signal photon and a laser photon. From the Lagrangian density, the wave equation of the signal light is obtained

$$(\partial_t^2 - \nabla^2)\mathbf{E}_S(t, \mathbf{x}) = 4\pi\mathbf{J}_V(t, \mathbf{x}), \quad (1)$$

Here the different components of the vacuum current vector determine the signals from vacuum birefringence and LBL scattering. It is known that the signal of ordinary

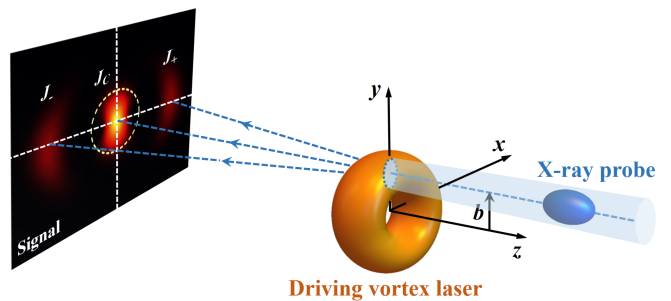


FIG. 1. Schematic layout of super-LBL scattering. An X-ray probe collides head-on, at the transverse impact parameter \mathbf{b} , with a driving laser pulse in a mixed vortex mode. The driving laser polarizes vacuum to generate the vortex vacuum current and induces photon-photon interaction. X-ray photons are scattered into signal photons by acquiring tangential momenta in azimuthal direction due to the local gradient force of the vortical vacuum current. Kicked out of the probe X-ray background (the yellow circle region on the screen), they form two detectable side-lobe signals.

LBL scattering cannot be directly measured in two-beam collision because the signal photons experience no momentum change. What can be detected is a birefringence signal with the aid of an X-ray polarizer or the LBL signals in three-beam collision, but in either case the weak signal will be further attenuated by at least two orders of magnitude. To boost the measurement efficiency and SNR, we propose a super-LBL scattering mechanism in the collision of an X-ray probe with a vortex driving laser. A phase vortex of a field possesses the phase factor $e^{il\theta}$, with l being the orbital angular momentum (OAM) projection of each quantum of this field. The gradient of this factor generates a local tangential momentum, $\mathbf{k}_\theta = \nabla_\theta e^{il\theta} = \frac{l}{r}\mathbf{e}_\theta$ [25]. A particle interacting with this vortex field is kicked in the azimuthal direction due to the transfer of the local momentum, which can exceed the transverse momentum of a quantum of the vortex field and is, therefore, referred to as the superkick [25–27].

We find that the superkick effect also exists in the quantum vacuum and leads to super-LBL scattering. Figure 1 presents a schematic layout of this process. We consider an ultra-intense driving laser pulse prepared in a mixed vortex mode (a superposition of two Laguerre-Gaussian (LG) modes with the OAM numbers l_1 and l_2) and an X-ray probe pulse colliding with it head-on, at the transverse impact parameter \mathbf{b} . The driving laser propagates along the $+z$ -direction, linearly polarized with polarization vector $(1/\sqrt{2})(\mathbf{e}_x + \mathbf{e}_y)$. To facilitate the distinction between the birefringent photons and LBL photons in the signals, we consider a linearly polarized Gaussian X-ray probe in y -direction. The polarization angle between them is $\pi/4$. Then the vacuum current is derived if we ignore the longitudinal component of the laser field,

$$\mathbf{J}_V(t, \mathbf{x}) \sim \xi j(t, \mathbf{x}) e^{-i(\omega x + k x z)} (-3\mathbf{e}_x + 11\mathbf{e}_y) + C.C. \quad (2)$$

The frequency and momentum of the X-ray are ω_X and $\mathbf{k}_X = (0, 0, -k_X)$. With the current (2), the wave equation (1) has an analytical solution in momentum space, with the signal light field $\mathbf{E}_S(t, \mathbf{k}_S)$. Then, the momentum distribution of the scattered signal photons normalized by the total energy of X-ray probe is derived, $dW(\mathbf{k}_S)/d^3\mathbf{k}_S = |\mathbf{E}_S(t, \mathbf{k}_S)|^2 / \int d^3\mathbf{x} |\mathbf{E}_X(t, \mathbf{x})|^2$, where $\mathbf{E}_X(t, \mathbf{x})$ is the electric field of the X-ray probe.

The \mathbf{e}_x -component of the vacuum current, Eq. (2), generates vacuum birefringent signals. The ratio of \mathbf{e}_x and \mathbf{e}_y components is 3/11, thus the number of birefringent signal photons accounts for at most 7% ($= 9/130$) of the total scattered photons. Here $j(t, \mathbf{x})$ is a scalar function determined by the pulse envelopes and the OAM numbers of the driving laser, which can be decomposed into three components: $j(t, \mathbf{x}) = j_C(t, \mathbf{x}) + j_+(t, \mathbf{x}) + j_-(t, \mathbf{x})$. $j_C(t, \mathbf{x})$ is vortex-independent; $j_{\pm}(t, \mathbf{x})$ are vortex-dependent and have the opposite vortex phases carrying the OAM numbers $\pm(l_1 - l_2)$. Then the induced vacuum current possesses, in addition to the main non-vortex component \mathbf{J}_C , two new vortex components, \mathbf{J}_+ and \mathbf{J}_- . They appear exclusively due to a non-zero overlap of the driving laser field with itself even if one transmits $\pm(l_1 - l_2)$ units of OAM from the driving field to an X-ray photon. These vortex components can be visualized as induced by absorption of a laser photon with the OAM l_1 (or l_2) and re-emitting it into a laser photon with the OAM l_2 (or l_1), see Supplemental Material for more information. They induce a local tangential momentum that is transferred to the scattered signal photons, and generate the super-LBL scattering. As it can be much larger than the momentum exchange in the standard VP effect, the signal photons are kicked out of the X-ray background, generating a directly measurable signal.

The super-LBL mechanism is demonstrated in Fig. 2. We consider the driving laser in a mixed vortex mode with two OAM numbers $l_1 = -l_2 = 10$. Figure 2(a) shows the laser modes and the Feynman diagrams of the super-LBL scattering, Fig. 2(b) presents the transverse momentum distribution of the scattered photons, $dW(\mathbf{k}_{S\perp})/d^2\mathbf{k}_{S\perp}$. The central bright spot corresponds to the ordinary LBL scattering, while the two side lobes displaced in the direction perpendicular to \mathbf{b} represent the hallmark signal of super-LBL scattering. Compared to the probe X-ray background, the momenta of LBL signals hardly changed, their distribution showing only slight broadening in the y -direction. However, their strength is ten orders of magnitude lower than that of the X-ray probe. Therefore, the LBL signals cannot be extracted from the X-ray background, unless an X-ray polarizer is used to detect the 7% birefringent signal. On the contrary, the super-LBL signals acquire a tangential momentum in the x -direction, which is nearly twice as much as the average transverse momentum of the driving LG laser $\langle k_{L\perp} \rangle$. This allows the signals to be clearly offset from the X-ray background with a high SNR. For comparison, we show the scattering of an X-ray probe with a driving LG laser in a single-vortex mode of $l = 10$ (Fig. 2(c) and

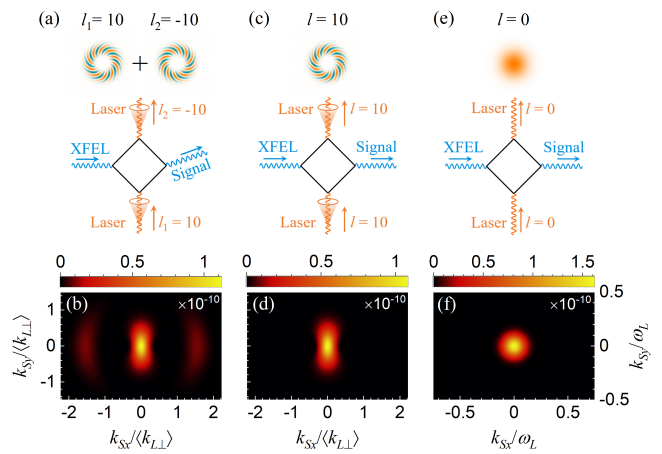


FIG. 2. Transverse momentum distributions of the signal photons. The driving laser is in coherent superposition mode of two vortex components with OAMs $l_1 = -l_2 = 10$ (a), single vortex mode with OAM $l = 10$ (c) and Gaussian mode (e), the Feynman diagrams of the photon-photon scattering are also shown in these figures. (b), (d) and (f) The corresponding transverse momentum distributions of the signal photons, $dW(\mathbf{k}_{S\perp})$. The wavelength of the driving laser is $\lambda_L = 800$ nm, focal spot waist $w_L = 2.2$ μm , peak intensity $I_L = 1 \times 10^{23}$ W/cm², and duration $\tau_L = 15$ fs. The photon energy of the X-ray probe is $\omega_X = 10$ keV, duration $\tau_X = 20$ fs, and focal spot $w_X = 3$ μm . The impact parameter is $b_x = 0$ and $b_y = 5$ μm .

(d) and with a Gaussian laser pulse (Fig. 2(e) and (f)). In both cases, the transverse momentum distributions of the signal photons feature only one central bright spot corresponding to LBL scattering.

Measurable signal analysis—Turning to the question of feasibility of experimental observation of super-LBL scattering, we need to address two issues. 1) Enough signal photons must be generated for the signal to be detected. 2) The signal photons must receive sufficient tangential momentum to be offset from the X-ray background and produce a high SNR, $\nu = N_{X,total} dW(\mathbf{k}_S) / dN_X(\mathbf{k}_X)$, where $N_X(\mathbf{k}_X)$ and $N_{X,total}$ are the momentum distribution and the total photon number of the X-ray probe. By performing the $dk_{Sy} dk_{Sz}$ integration of $dW(\mathbf{k}_S)$, we compare the tangential momentum distribution of the signal photons with the probe X-ray background for various collision parameters b in Fig. 3(a). The central peaks of the blue lines are the signals of LBL scattering, and the two side peaks are the super-LBL signals. We find that the LBL signals are obscured by the X-ray background (orange areas), while the super-LBL signals are kicked out and distinctly visible. The signals are strongest when the collision parameter is around $b_y = 5$ μm , which corresponds to the focal spot size of the driving laser. Figure 3(b) shows the tangential momentum distribution of the signal photons for $b_y = 5$ μm , where the blue shading is the area with SNR $\nu > 100$. This indicates that the SNR of the super-LBL signals is very large.

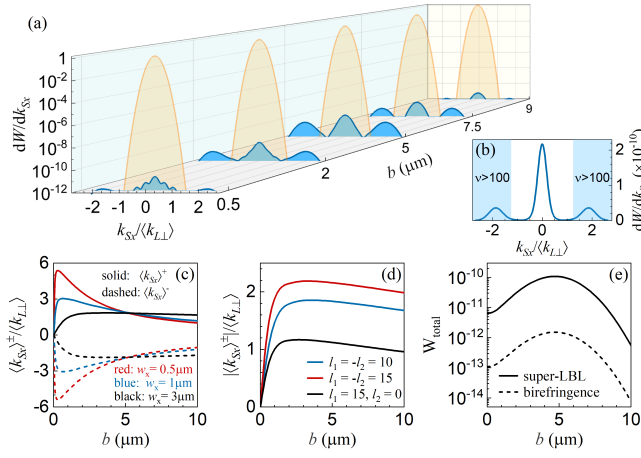


FIG. 3. Analysis of the observable signals. Tangential momentum distributions of signal photons for various collision parameters \mathbf{b} (a) and for $b_y = 5 \mu\text{m}$ with SNR $\nu > 100$ (blue shading area) (b). Average tangential momenta $\langle k_{Sx} \rangle^\pm$ of the super-LBL signals for various X-ray focal spot size (c) and for various vortex modes of driving laser. (e) Peak numbers of the super-LBL signals and birefringent signal versus the collision parameter b .

We calculate the average value of the tangential momentum of the super-LBL signal photons $\langle \mathbf{k}_{S\perp} \rangle$ as $\langle \mathbf{k}_{S\perp} \rangle^\pm = \int d^3 \mathbf{k}_S \mathbf{k}_{S\perp} |\mathbf{E}_\pm(\mathbf{k}_S)|^2 / \int d^3 \mathbf{k}_S |\mathbf{E}_\pm(\mathbf{k}_S)|^2$. Since the impact parameter \mathbf{b} is along the y -axis, it can be demonstrated that $\langle \mathbf{k}_{S\perp} \rangle$ is directed along the x -axis: $\langle k_{Sy} \rangle^\pm = 0$. Figure 3(c) shows $\langle k_{Sx} \rangle^\pm$ of the super-LBL signals for various X-ray focal spots normalized to the average transverse momentum of the driving LG laser $\langle k_{L\perp} \rangle$. The “ \pm ” modes are symmetrically distributed, and $\langle k_{Sx} \rangle^\pm$ can be several times larger than $\langle k_{L\perp} \rangle$, the feature that justifies the term super-kick. Roughly, $\langle k_{Sx} \rangle^\pm$ is inversely proportional to the collision parameter \mathbf{b} . But as \mathbf{b} approaches 0, $\langle k_{Sx} \rangle^\pm$ drops rapidly [25]. Considering the size of the laser focal spot, the tangential momentum is an average result of the phase tangential force over the overlapping area of focal spots of driving laser and X-ray probe. This means the signal photons could sense the local gradient force more accurately and gain larger tangential momentum if the X-ray focal spot is smaller. We also compare in Fig. 3(d) the magnitude of $|\langle k_{Sx} \rangle^\pm|$ in different driving LG modes and confirm its proportionality to the OAM number of the vacuum current, $\Delta l = \pm(l_1 - l_2)$. In principle, if the vacuum current carries a sufficiently high OAM and the collision point is close to the central phase singularity, the gradient and local momentum will be large. However, considering the hollow structure of the vortex light, we cannot collide the X-ray pulse too close to the phase singularity of the driving laser to attain larger gradient force. Nevertheless, by manipulating the mode of the driving laser and its focal spot size, we can still generate a prominent tangential momentum to kick the signal photons out of the X-ray background.

The signal photon number is calculated by integrating the momentum distribution $N_S = \int dW(\mathbf{k}_S)$. In Fig. 3(e), we show the total photon number of the super-LBL signals normalized to the X-ray probe photon number as a function of the collision parameter, see the solid line. The peak value reaches 1.1×10^{-10} at $b_y = 5 \mu\text{m}$. If the X-ray probe contains $N_X = 10^{12}$ photons, more than 100 signal photons are kicked out and experimentally detectable with SNR $\nu > 100$. The full width at half maximum is about $3.8 \mu\text{m}$, which determines the transverse alignment accuracy goal of the two lasers in experiment. For comparison, we calculate the measurable photon number of birefringent signals in the central peaks in Fig. 3(a). Considering the transmission efficiency of the X-ray polarizer is 10% [20], the measurable number of the birefringent signals is attenuated by two orders of magnitude, see the dashed line in Fig. 3(e), significantly lower than the super-LBL signals. And its SNR is also less than 1, as the measurable signal strength is below the detection accuracy of the polarizer. These results indicate that super-LBL scattering can generate enough measurable signals with a high SNR in the collision of an ultra-intense laser with an X-ray pulse, for example the 100 PW laser and 10 keV XFEL in SEL at SHINE [16]. This effect opens up new opportunities for detecting the VP effect with the present-day intense laser and XFEL technologies. It even allows for single-shot detection.

Experimental scheme—It remains to be shown how to produce an ultra-intense laser pulse in two-vortex mixed mode. We propose a feasible scheme presented in Fig. 4(a). An intense laser pulse interacts with a special designed double-ring spiral phase plate (DSPP) and is modulated into a two-vortex mixed mode. The structure of the DSPP is shown in Fig. 4(b), it is divided into the inner and outer circles, which may have different spiral steps to modulate the laser mode. The height of each step H is half the laser wavelength, $H = \lambda_L/2$. In Fig. 4(b) the step number of the DSPP in both the inner and outer circles is 10, but their directions are opposite. When interacting with this DSPP, the laser pulse is converted into two vortex modes in inner and outer circles with OAMs $l_1 = 10$ and $l_2 = -10$. After reflection from DSPP, the two vortex modes overlap during propagation, producing a mixed vortex laser pulse. The reflected laser is focused by a parabolic mirror and then collides with an X-ray probe to trigger super-LBL scattering and generate the measurable signals, see Fig. 4(c). We confirmed the effectiveness of this DSPP-based modulating scheme through three-dimensional (3D) PIC simulation. A y -polarized incident laser propagates along z -axis, its wavelength is $\lambda_L = 800 \text{ nm}$ and transverse envelope is super-Gaussian. Figure 4(d) shows the OAM spectrum of the reflected laser, which is dominated by the $l = \pm 10$ modes. The electric fields E_y of these two modes in xy plane are shown in Fig. 4(e) and (f). They possess nearly identical strengths and focal radii, indicating that the reflected laser is a coherent superposition of two OAM modes with $l_1 = 10$ and $l_2 = -10$. Therefore, the sim-

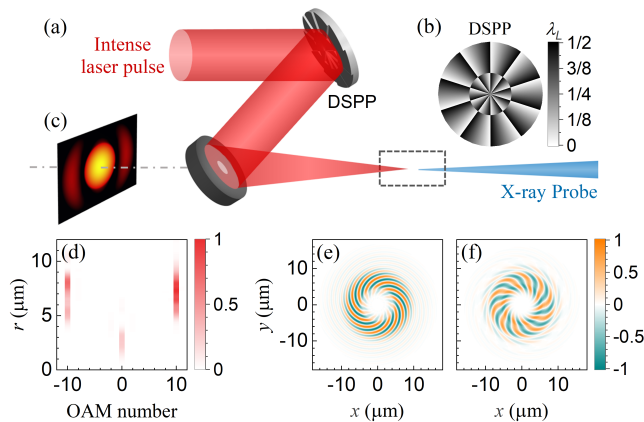


FIG. 4. (a) The proposed experimental scheme for detecting the super-LBL scattering. (b) The structure of DSPP. The step number in both the inner and outer circles of the DSPP is 10, but their directions are opposite. (c) The transverse distribution of the signal photons and the probe X-ray background after the vortex-laser-XFEL interaction. (d) The OAM spectrum of the reflected laser field. (e) and (f) The electric fields E_y of the two vortex modes in transverse plane.

ulation demonstrates the possibility of experimental detection of super-LBL scattering.

Conclusion and outlook—We theoretically discovered a novel QED VP effect, super-LBL scattering, which is driven by an ultra-intense vortex laser in a superposition of two OAM modes. We find that the vortical vacuum current generates a large local tangential momentum,

which is transferred to the scattered photons and kicks them out of the probe X-ray background. The scheme does not rely on X-ray polarizers and the associated signal attenuation, avoids the complexity of the three-beam collision setting, and reduces the requirements for spatiotemporal alignment accuracy. With a 3D PIC simulation, we argue that ultra-intense two-vortex mixed laser necessary for super-LBL scattering can be generated by using a DSPP. We find that super-LBL scattering can generate enough signal photons and a high SNR > 100 , both figures exceeding the vacuum birefringence and three-beam LBL scattering counterparts by at least two orders of magnitude. Not only do we propose this phenomenon as a means to detect the long-predicted nonlinear VP effects, but we argue that it can be done in a single shot experiment with the present-day intense laser and XFEL technologies. Realization of this idea will help verify QED processes in the extremely nonlinear regime and will reveal the quantum nature of the QED vacuum in an ultra-intense field.

Acknowledgments—This work was supported by the National Science Foundation of China (Grant Nos. 12388102, 24G0011101), the Strategic Priority Research Program of Chinese Academy of Sciences (No. XDB0890303), the CAS Project for Young Scientists in Basic Research (Grant No. YSBR060), and the National Key R&D Program of China (Grant No. 2022YFE0204800).

Corresponding author:

*ivanov@mail.sysu.edu.cn

†jill@siom.ac.cn

-
- [1] W. Heisenberg and H. Euler, *Z. Phys.* **98**, 714 (1936).
 [2] J. J. Klein and B. P. Nigam, *Phys. Rev.* **135**, B1279 (1964).
 [3] Z. Bialynicka-Birula and I. Bialynicki-Birula, *Phys. Rev. D* **2**, 2341 (1970).
 [4] T. Heinzl, B. Liesfeld, K.-U. Amthor, H. Schworer, R. Sauerbrey, and A. Wipf, *Opt. Commun.* **267**, 318 (2006).
 [5] F. Moulin and D. Bernard, *Opt. Commun.* **164**, 137 (1999).
 [6] E. Lundström, G. Brodin, J. Lundin, M. Marklund, R. Bingham, J. Collier, J. T. Mendonça, and P. Norreys, *Phys. Rev. Lett.* **96**, 083602 (2006).
 [7] A. D. Piazza, K. Z. Hatsagortsyan, and C. H. Keitel, *Phys. Rev. Lett.* **97**, 083603 (2006).
 [8] B. King, A. D. Piazza, and C. H. Keitel, *Nat. Photon.* **4**, 92 (2010).
 [9] P. Böhl, B. King, and H. Ruhl, *J. Plasma Phys.* **82**, 655820202 (2016).
 [10] H. Kadlecová, G. Korn, and S. V. Bulanov, *Phys. Rev. D* **99**, 036002 (2019).
 [11] J. Schwinger, *Phys. Rev.* **82**, 664 (1951).
 [12] C. Hernandez-Gomez, S. P. Blake, O. Chekhlov, R. J. Clarke, A. M. Dunne, M. Galimberti, S. Hancock, R. Heathcote, P. Holligan, A. Lyachev, P. Matousek, I. O. Musgrave, D. Neely, P. A. Norreys, I. Ross, Y. Tang, T. B. Winstone, B. E. Wyborn, and J. Collier, *J. Phys.: Conf. Ser.* **244**, 032006 (2010).
 [13] F. Lureau, S. Laux, O. Casagrande, O. Chalus, A. Pellegrina, G. Matras, C. Radier, G. Rey, S. Ricaud, S. Herriot, P. Jouglu, M. Charbonneau, P. A. Duvochelle, and C. Simon-Boisson, *Proc. SPIE* **9726**, 972613 (2016).
 [14] B. L. Garrec, D. N. Papadopoulos, C. L. Blanc, J. P. Zou, G. Chériaux, P. Georges, F. Druon, L. Martin, L. Fréneaux, A. Beluze, N. Lebas, F. Mathieu, and P. Audebert, *Proc. SPIE* **10238**, 102380Q (2017).
 [15] W. Li, Z. Gan, L. Yu, C. Wang, Y. Liu, Z. Guo, L. Xu, M. Xu, Y. Hang, Y. Xu, J. Wang, P. Huang, H. Cao, B. Yao, X. Zhang, L. Chen, Y. Tang, S. Li, X. Liu, S. Li, M. He, D. Yin, X. Liang, Y. Leng, R. Li, and Z. Xu, *Opt. Lett.* **43**, 5681 (2018).
 [16] B. Shen, Z. Bu, J. Xu, T. Xu, L. Ji, R. Li, and Z. Xu, *Plasma Phys. Control. Fusion* **60**, 044002 (2018).
 [17] N. Ahmadiaz and C. B. et al. (BIREF@HIBEF Collaboration), (2024), arXiv: 2405.18063.
 [18] F. Karbstein and C. Sundqvist, *Phys. Rev. D* **94**, 013004

- (2016).
- [19] B. Marx, K. S. Schulze, I. Uschmann, T. Kämpfer, R. Löttsch, O. Wehrhan, W. Wagner, C. Detlefs, T. Roth, J. Härtwig, E. Förster, T. Stöhlker, and G. G. Paulus, *Phys. Rev. Lett.* **110**, 254801 (2013).
- [20] S.-Y. Si, Z.-L. Li, W.-H. Jia, L. Xue, H.-X. Luo, J.-C. Xu, B.-F. Shen, L.-G. Zhang, L.-L. Ji, Y.-X. Leng, and R.-Z. Tai, *Nucl. Sci. Tech.* **35**, 51 (2024).
- [21] K. S. Schulze and B. G. et al., *Phys. Rev. Research* **4**, 013220 (2022).
- [22] F. Karbstein, D. Ullmann, E. A. Mosman, and M. Zept, *Phys. Rev. Lett.* **129**, 061802 (2022).
- [23] H. Gies, F. Karbstein, C. Kohlfürst, and N. Seegert, *Phys. Rev. D* **97**, 076002 (2018).
- [24] N. Ahmadieniaz, T. E. Cowan, J. Grenzer, S. Franchino-Viñas, A. L. Garcia, M. Šmíd, T. Toncian, M. A. Trejo, and R. Schützhold, *Phys. Rev. D* **108**, 076005 (2023).
- [25] S. M. Barnett and M. V. Berry, *J. Opt.* **15**, 125701 (2013).
- [26] A. Afanasev, C. E. Carlson, and A. Mukherjee, *Phys. Rev. Research* **3**, 023097 (2021).
- [27] Z. Li, S. Liu, B. Liu, L. Ji, and I. P. Ivanov, *Phys. Rev. Lett.* **133**, 265001 (2024).